molecular pharmaceutics

Article

Cite This: Mol. Pharmaceutics 2018, 15, 4202−4213

pubs.acs.org/molecularpharmaceutics

Mechanism of Binding of Antifungal Antibiotic Amphotericin B to Lipid Membranes: An Insight from Combined Single-Membrane Imaging, Microspectroscopy, and Molecular Dynamics

Ewa Grela,[†,‡,□] Miłosz Wieczór,[§,□] Rafał Luchowski,[†] Joanna Zielinska,[∥] Angelika Barzycka,[†] Wojciech Grudzinski,[†] Katarzyna Nowak,[⊥] Piotr Tarkowski,[¶] Jacek Czub,*[,§] and Wieslaw I. Gruszecki*[,†]

[†]Department of Biophysics, Institute of Physics, Maria Curie-Sklodowska University, 20-031 Lublin, Poland

[‡]Department of Biophysics, Institute of Biology, Maria Curie-Sklodowska University, 20-031 Lublin, Poland

[§]Department of Physical Chemistry, Gdansk University of Technology, 80-233 Gdansk, Poland

[∥]Department of Pharmaceutical Chemistry, Medical University of Gdansk, 80-416 Gdansk, Poland

[⊥]Department of Natural Environment Biogeochemistry, Institute of Agrophysics, Polish Academy of Sciences, 20-290 Lublin, Poland

[¶]Medical University of Lublin, 20-059 Lublin, Poland

S *Supporting Information*

ABSTRACT: Amphotericin B is a lifesaving polyene antibiotic used in the treatment of systemic mycoses. Unfortunately, the pharmacological applicability of this drug is limited because of its severe toxic side effects. At the same time, the lack of a well-defined mechanism of selectivity hampers the efforts to rationally design safer derivatives. As the drug primarily targets the biomembranes of both fungi and humans, new insights into the binding of amphotericin B to lipid membranes can be helpful in unveiling the molecular mechanisms underlying both its pharmacological activity and toxicity. We use fluorescence-lifetime-imaging microscopy combined with fluorescence-emission spectroscopy in the microscale to study the interaction of amphotericin B with single lipid bilayers, using model systems based on giant unilamellar liposomes formed with three lipids: dipalmitoylphosphatidylcholine (DPPC), dimirystoylphosphatidylcholine (DMPC), and 1-palmitoyl-2-oleoylphosphatidylcholine (POPC). The results show that amphotericin B introduced into the water phase as a DMSO solution binds to the membrane as dimers and small-molecular aggregates that we identify as tetramers and trimers. Fluorescence-detected linear-dichroism measurements revealed high orientational freedom of all the molecular-organization forms with respect to the membrane plane, which suggests that the drug partially binds to the membrane surface. The presence of sterols in the lipid phase (cholesterol but particularly ergosterol at 30 mol %) promotes the penetration of drug molecules into the lipid membrane, as concluded on the basis of the decreased orientation angle of amphotericin B molecules with respect to the axis normal to the membrane plane. Moreover, ergosterol facilitates the association of amphotericin B dimers into aggregated structures that can play a role in membrane destabilization or permeabilization. The presence of cholesterol inhibits the formation of small aggregates in the lipid phase of liposomes, making this system a promising candidate for a low-toxicity antibiotic-delivery system. Our conclusions are supported with molecular simulations that reveal the conformational properties of AmB oligomers in both aqueous solution and lipid bilayers of different compositions.

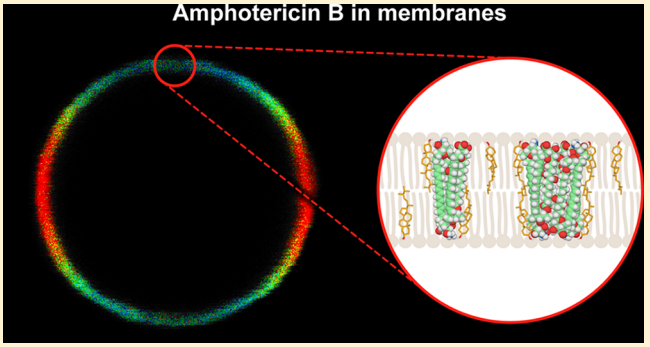

KEYWORDS: *amphotericin B, polyene antibiotics, antimycotic therapy, bioimaging, GUV*

INTRODUCTION

Amphotericin B (AmB, see Supplementary Figure S1 for the chemical structure) is a polyene antibiotic used as a gold standard in the treatment of deep-seated, life-threatening mycotic infections.[1] The antibiotic has been in use for several decades, despite severe side effects, because of its high

Received: June 1, 2018
Revised: July 21, 2018
Accepted: August 6, 2018
Published: August 6, 2018

DOI: 10.1021/acs.molpharmaceut.8b00572
Mol. Pharmaceutics 2018, 15, 4202−4213

pharmacological efficacy.[2] Numerous research groups worldwide are working to unveil the molecular mechanisms underlying the toxicity of AmB to ultimately engineer a pharmacological formula of the drug with minimized toxic side effects and retained or enhanced antifungal activity.[3−5] According to a general conviction, the selectivity of AmB toward fungi is based upon the stronger interaction of the drug molecules with ergosterol (Ergo), present in the membranes of fungi, as compared with its interaction with cholesterol (Chol), the sterol of the biomembranes of human cells.[6−8] Unlike the mostly consistent views and opinions on the selectivity of AmB, the concepts on the possible modes of action and even the localization of drug molecules within lipid membranes are quite different or even contradictory. On the one hand, AmB is postulated to form transmembrane pores in lipid membranes,[9−11] but on the other hand, the biological activity of the drug is believed to be based upon sequestration of sterols from biomembranes and formation of extramembranous sterol sponges.[12] In principle, both postulated mechanisms can directly or indirectly affect membrane transport by changing the physical properties of the lipid bilayers and therefore their ion permittivity.[13−15] It is very likely that both the formation of transmembrane pores and the selective binding of membrane sterols by AmB molecules (either intra- or extramembranous) play a biological role under physiological conditions. The results of the recent studies show that AmB molecules immobilized at the surface of silver nanoparticles and therefore unable to self-organize into ionic pores inside a membrane are highly effective antifungal agents.[16] It also was shown that such hybrid AmB−silver nanoparticles are not cytotoxic with respect to human cells,[16] which suggests a selective interaction of the nanoparticle-bound drug molecules with Ergo. On the other hand, it was also shown that the presence of Ergo in giant unilamellar vesicles (GUV) enabled the incorporation of AmB molecules into the lipid phase as well as their self-organization into small supramolecular structures.[17] The results of those studies strongly indicate that both proposed molecular mechanisms, sequestration of Ergo and formation of intramembrane supramolecular structures composed of sterol and AmB molecules, play a role in the case of sterol-rich lipid membranes. The intriguing question is whether the exact mode of action of AmB, including the toxic side effects, depends on the way in which drug molecules are delivered to biomembranes. In most model-membrane studies, AmB molecules were mixed with lipids and sterols upon lipid-bilayer formation. In the present work, molecular organization of AmB in the lipid-membrane-model systems is analyzed after injection of a solution of the drug in DMSO into the water phase of a suspension of preformed membranes. Such an approach models the process of delivery of the antibiotic to natural biomembranes of living organisms in a more realistic way. Application of fluorescence-microscopy techniques with respect to individual GUV structures enabled precise analyses of the molecular organization of AmB in a single lipid bilayer, filtering out any effects originating from drug aggregates formed in the water phase. Our analyses and conclusions are supported with molecular simulations that reveal the conformational properties of AmB oligomers in both the aqueous solution and lipid bilayers of different compositions.

MATERIALS AND METHODS

Materials. Antibiotic amphotericin B from *Streptomyces* sp. (AmB), 1,2-dipalmitoyl-*sn*-glycero-3-phosphocholine (DPPC), 1,2-dimyristoyl-*sn*-glycero-3-phosphocholine (DMPC), cholesterol (Chol), ergosterol (Ergo), tricine, and dimethyl sulfoxide (DMSO) were purchased from Sigma-Aldrich Chemical Company. 1-Palmitoyl-2-oleoyl-*sn*-glycero-3-phosphocholine (POPC) was purchased from Avanti Polar Lipids Inc. Ethanol, chloroform, 2-propanol, and potassium chloride (KCl) were of analytical purity and were obtained from POCH. Water used during all the experiments was purified by a Milli-Q system from Merck Millipore.

Experimental Methods. Amphotericin B (AmB) was dissolved in chloroform−water (1:1, v/v), then vortexed for 30 min, collected from the interphase, and evaporated under nitrogen. Dry AmB was suspended in 2-propanol−water (4:6, v/v) and centrifuged for 5 min at 14 000*g* to remove crystals of the antibiotic. Finally, the AmB solution was purified by HPLC on a C18 reversed-phase column (250 × 4.6 mm) with a 2-propanol−water (4:6, v/v) mobile phase.

Giant unilamellar liposomes were formed of either pure lipids or the lipids with either cholesterol or ergosterol at 30 mol %. The procedure of formation of the giant unilamellar vesicles (GUV) was described previously in detail.[17] AmB in a DMSO solution was added to the buffer after 1 h of electroformation. The final drug concentration was 0.5 mol % with respect to the phospholipid. The temperature at the time of electroformation was maintained above the main phase transition (at 50 °C for membranes formed with DPPC, at 30 °C in the case of membranes formed with DMPC, and at 24 °C in the case of the membranes formed with POPC). The final concentration of DMSO in the liposome suspensions was 0.7%, below the level reported to modify the structural properties of lipid membranes.[18,19] The DSC tests were also performed with the lipid systems studied, in which pure DMSO solution was added to the samples instead of AmB solutions. The results have confirmed that DMSO addition at the concentration applied did not significantly affect lipid-membrane thermotropic properties, in accordance with the literature data.[18]

Absorption spectra were recorded with a Cary 60 UV−vis spectrophotometer (Agilent Technologies). A concentration of AmB was established on the basis of the molar-extinction coefficient (130 000 M^{-1} cm^{-1}) at 408 nm absorption maximum. Fluorescence-emission spectra were recorded with the application of a Cary Eclipse fluorescence spectrophotometer (Varian). Fluorescence-excitation and -emission bandwidths were set to 5 nm.

Microscopy measurements were carried out on a MicroTime 200 confocal system from PicoQuant GmbH connected to an Olympus IX71 inverted microscope. The samples were excited by a 405 nm pulsed laser with a 10 MHz repetition rate. The time resolution was set to 16 ps. The experiments were carried out with the application of a water-immersed objective (Olympus NA = 1.2, 60×). The observations were performed in the confocal configuration using a pinhole of 50 μm in diameter and proper optics based on a ZET405 StopLine Notch Filter, a ZT 405RDC dichroic filter, and 430 nm long wavelength pass filter from Chroma-AHF Analysentechnik. The fluorescence signal was divided by a polarizing cube to measure parallel and perpendicular intensities by two identical detectors (Single Photon Avalanche Diodes). The fluorescence lifetimes and anisotropies were analyzed using the SymPhoTime 64 v. 2.1 software (PiqoQuant).

The size of the pinhole applied in the confocal system was selected to afford both a reasonable emission signal from the

DOI: 10.1021/acs.molpharmaceut.8b00572
Mol. Pharmaceutics 2018, 15, 4202−4213

GUVs and a very small confocal volume to slice the measured objects. On the basis of separate measurements performed for the 405 nm excitation and detection parts aligned identically for all the measurements, the effective confocal volume was calculated to be 0.32 fl. The value has been established on the basis of measurements performed for fluorescent beads 30 nm diameter (much below the optical-resolution limit). Ellipsoid's X, Y, and Z dimensions were measured to be 252 ± 9, 255 ± 5, and 902 ± 26 nm, respectively.

The intensity decays for each sample were fitted with the multiexponential model:

$$I(t) = \sum_i \alpha_i \exp(-t/\tau_i)$$

where τ_i is the decay time, and α_i is the relative amplitude of each individual component ($\sum \alpha_i = 1$). The amplitude-weighted average lifetime was calculated on the basis of the following formula:[20]

$$\langle \tau \rangle = \sum_i \alpha_i \tau_i$$

Lifetime data from single GUV structures were collected simultaneously with fluorescence-emission spectra by a Shamrock 163 spectrograph attached to the microscopy system. The detection was based on a Newton EMCCD DU970P BUF camera (Andor Technology) cooled to −50 °C.

A microCal VP-Capillary DSC microcalorimeter from General Electric Healthcare, supported by the VPViewer2000 software, was used to conduct calorimetric measurements. In order to run DSC measurements, a GUV suspension was subjected to centrifugation for 3 min at 7000g, and a sediment was transferred into a measuring cell (a volume of 209 μL). During measurements, the pressure was stabilized at 26.89 × 10^4 Pa. Samples were scanned against the degassed pure buffer, as a control. A test experiment, in which buffer samples were placed in both the measuring and reference cells, was conducted for each condition, and the thermograms recorded were subtracted from the thermograms recorded for liposome-containing samples. The scan rate was 1 °C/min with a temperature range of 30−50 °C for liposomes formed with DPPC and 15−40 °C for liposomes formed with DMPC. Cells were thermostated for 10 min before each measurement. At least three DSC measurements were conducted, representing different preparations of all the systems studied, and the thermograms recorded were found to be highly reproducible.

Molecular Dynamics. Models of lipid-bilayer systems with three different structures of AmB tetramers were prepared in the CHARMM-GUI Membrane Builder.[21] Three AmB tetramers were composed of four parallel-oriented monomers (4−0), two antiparallel dimers (2−2), or one parallel and one antiparallel dimer (3−1) and placed in a lipid bilayer. Systems were embedded in 82.03 × 82.03 × 121.09 rectangular boxes and were composed of 190 DMPC and 82 Ergo molecules (model fungal membrane) or 190 DMPC molecules (model bacterial membrane). Then, 18 550 TIP3 water molecules, 54 K^+, and 54 Cl^- ions were added to solvate the systems and obtain physiological ionic strength (0.15 M). In the case of the 4−0 tetramer, analogous systems were prepared that contained (1) DPPC, (2) DPPC with Ergo, (3) DPPC with Chol, (4) DMPC, (5) DMPC with Ergo, and (6) DMPC with Chol. AmB trimers were then obtained by pulling a single AmB molecule away from the tetramer; this was performed by increasing the minimum distances between the selected molecule and the remaining three molecules from 0.25 to 0.7 nm using the Plumed plugin.[22] Simulations of AmB tetramers in the water phase were taken from our previous study.[23] The Charmm36 force field[24] was applied for lipids and sterols, and AmB molecules were modeled using a previously validated set of parameters.[6,11,23,25]

All energy minimizations and molecular-dynamics simulations were performed in Gromacs 5.0.4.[26] The simulations were performed in the NPT ensemble. The v-rescale thermostat with a coupling time of 5 ps was used to keep the temperature at 315 K, and the semi-isotropic Berendsen barostat with a coupling time of 2 ps was used to keep the pressure at 1 bar.[27] The Verlet leapfrog algorithm with a time step of 2 fs was applied to integrate the equations of motion.[28]

Bond lengths were constrained using P-LINCS,[29] and the SETTLE algorithm[30] was used for water molecules. To calculate electrostatic interactions, particle-mesh Ewald summation was applied with a real-space cutoff of 1.2 nm and a Fourier grid spacing of 0.12 nm.[31]

Equilibrium properties were analyzed using at least 300 ns production runs per system. The solvent-accessible surfaces (SASAs) for the conjugated double bonds (polyene) were calculated using gmx sasa from the Gromacs package, whereas distance and angle distributions were calculated using the MDTraj library.[32] Convergence was assumed when the time series of the parameters of interest (i.e., SASA and interchromophore distance) reached a plateau, which typically took from 50 (in water phase) to 200−500 ns (in lipid bilayers). Principal-component analysis (PCA) was performed using an aggregated set of all tetramers' simulations in DPPC as training data, with the distribution-of-reciprocal-interatomic-distances (DRID) featurizer of MSMBuilder employed to transform the original Cartesian coordinates. All molecular visualizations were prepared using VMD.[33]

RESULTS

We first investigated the molecular organization of AmB at the two stages of direct delivery of the drug to lipid membranes. Figure 1 shows a comparison of the absorption and fluorescence spectra of AmB introduced in the form of a DMSO solution into the buffer medium and into the suspension of liposomes. The pronounced differences in the spectra represent differences in the molecular organization of the drug in both systems, primarily owing to the interaction of AmB molecules with lipid membranes. The striking difference is an intense absorption maximum in the short-wavelength region (peaking at 332 nm) representing molecular aggregates of AmB[34] that are formed efficiently in the water phase but are present at a relatively lower extent in the experimental system containing lipid membranes. In order to analyze molecular forms of AmB involved directly in interactions with lipid membranes, we employed microscopic analyses of single unilamellar lipid vesicles, based on fluorescence-lifetime imaging (FLIM) and steady-state fluorescence-emission spectroscopy on a microscale. Figures 2−4 show FLIM images of individual, AmB-containing GUVs formed with three lipids (DPPC, DMPC, and POPC) and images of vesicles formed with the same lipids but also containing 30 mol % sterols, either Chol or Ergo, in order to model biomembranes of human and fungal cells, respectively. Fluorescence-anisotropy images are also presented, along with the fluorescence-lifetime images, to reveal the orientation of AmB molecules with respect to the plane of the lipid membrane.[17] Detailed values of

DOI: 10.1021/acs.molpharmaceut.8b00572
Mol. Pharmaceutics 2018, 15, 4202−4213

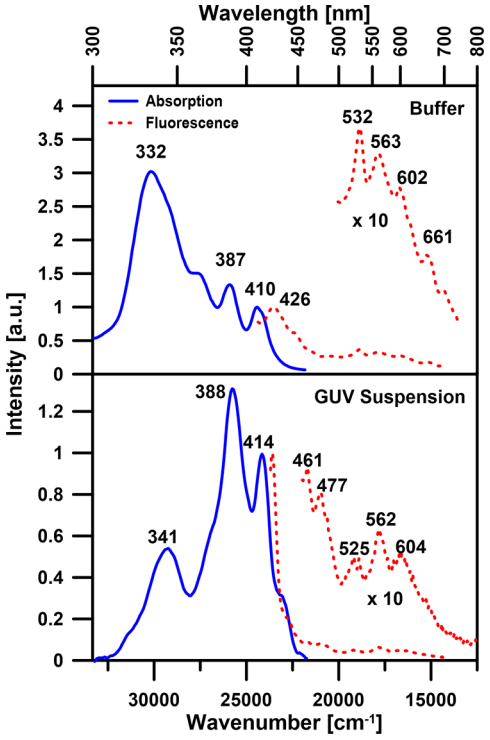

Figure 1. Absorption and fluorescence-emission spectra of AmB in the buffer and in the liposome suspension. A solution of AmB in DMSO was injected into the water phase (upper panel) or into a suspension of giant unilamellar liposomes formed with DMPC (lower panel). The experiment was performed and the spectra recorded at 25 °C, above the main phase transition of the lipid. The absorption spectra were calculated as 1 minus the transmission ($1 - T$). All the spectra presented were normalized at the maximum close to 400 nm. The long-wavelength parts of the fluorescence-emission spectra are also shown on a magnified scale. The positions of the selected absorption and emission maxima are marked (presented in nanometers).

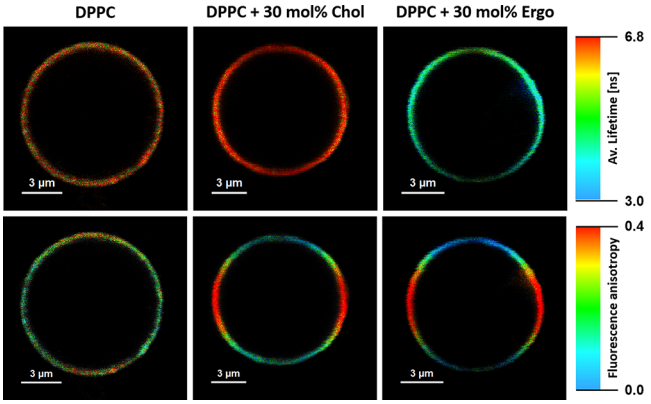

Figure 2. Results of microscopic imaging of single lipid vesicles composed of DPPC and containing amphotericin B. The images are based on fluorescence lifetimes (upper row) and fluorescence anisotropy (lower row). The three panels show liposomes formed with pure DPPC, DPPC with 30 mol % Chol, and DPPC with 30 mol % Ergo (indicated). The images represent an equatorial vesicle cross-section in the focal plane of the microscope. Maximum fluorescence-anisotropy values (displayed in red) on the left and right sides of the liposomes represent the fraction of molecules perpendicular to the membrane plane (e.g., in the cases of DPPC+Ergo and DPPC+Chol), whereas the fractions oriented parallel to the membrane are represented by red in the upper and lower portions of the liposome images (e.g., in the case of pure DPPC).

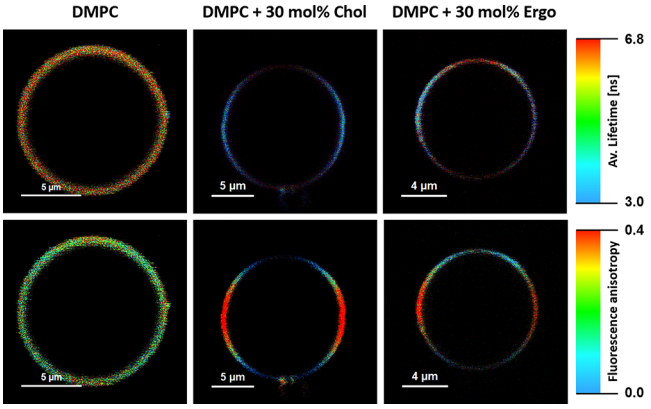

Figure 3. Results of microscopic imaging of single lipid vesicles composed of DMPC and containing AmB. The images are based on fluorescence lifetimes (upper row) and fluorescence anisotropy (lower row). Three panels show liposomes formed with pure DMPC, DMPC with 30 mol % Chol, and DMPC with 30 mol % Ergo (indicated). The images represent an equatorial vesicle cross-section in the focal plane of the microscope. Maximum fluorescence-anisotropy values (displayed in red) on the left and right sides of the liposomes represent the fraction of molecules perpendicular to the membrane plane (e.g., in the case of DMPC+Chol), whereas the fractions oriented parallel to the membrane are represented by red in the upper and lower portions of the liposome images (e.g., in the case of pure DMPC).

the average orientation of the transition dipole axis of AmB in the lipid bilayers of all the systems studied, determined on the basis of the fluorescence images,[17] are presented in Table 1. As can be seen from Table 1, the average orientation of the small aggregated structures of AmB, represented by the relatively short fluorescence-lifetime component (below 1 ns) in the membranes formed with pure lipids is very close to the magic angle (54.7°). This is consistent with the high orientational freedom of the molecules and the lack of any distinguished orientation of the AmB structures relatively weakly bound at the membrane-surface layer, as strongly supported by our MD simulations (see Figure 5 and discussion below) as well as previous reports.[17] Importantly, the presence of sterols in the lipid phase is associated with a pronounced decrease in the orientation angle of aggregated structures of AmB, a shift that likely results from incorporation into the lipid phase. This is again confirmed by our MD simulations in which AmB molecules forming trimers and tetramers align themselves with the membrane-normal axis, particularly in sterol-rich membranes (see Figure 6), which is also in agreement with earlier studies.[17,25] This effect can also be clearly seen from the distribution of spectral forms, giving rise to high fluorescence-anisotropy values (Figures 2−4). Interestingly, the effect observed in the case of Ergo is not as clearly pronounced in the case of Chol, in particular in the membranes formed with POPC (Table 1). In this case, the presence of a sterol even shifts the average orientation angles of different spectral forms toward higher values. Such an effect can be diagnostic for the formation of molecular structures of the drug associated with the lipid-membrane-headgroup region and adopting a lateral orientation. Interestingly, the presence of sterols induced not only reorientation of AmB molecules but also a reorganization of molecular structures of the drug, as can be concluded on the

DOI: 10.1021/acs.molpharmaceut.8b00572
Mol. Pharmaceutics 2018, 15, 4202−4213

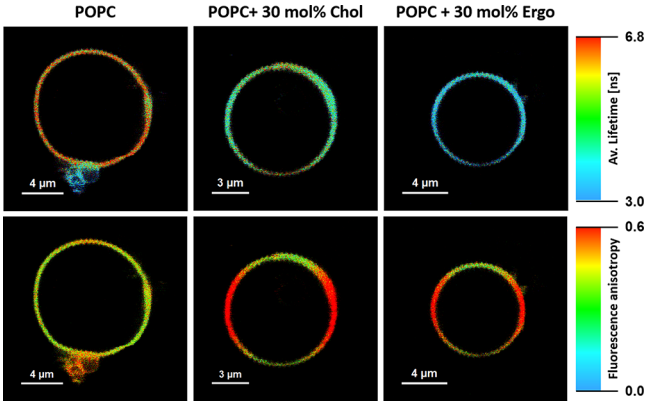

Figure 4. Results of microscopic imaging of single lipid vesicles composed of POPC and containing AmB. The images are based on fluorescence lifetimes (upper row) and fluorescence anisotropy (lower row). Three panels show liposomes formed with pure POPC, POPC with 30 mol % Chol, and POPC with 30 mol % Ergo (indicated). The images represent an equatorial vesicle cross-section in the focal plane of the microscope. See for Figure 3 further explanations. Notice the presence of the extramembranous AmB structure, visible in the case of pure POPC and characterized by low fluorescence lifetimes (appearing in blue) and high fluorescence anisotropy (appearing in red).

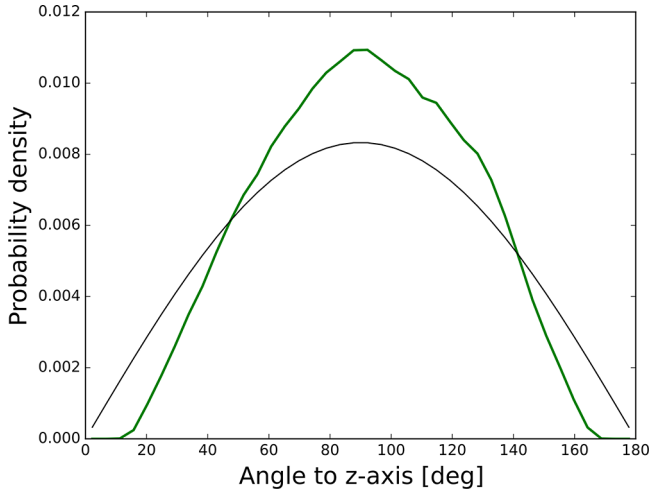

Figure 5. Orientation of AmB oligomers in the vicinity of the membrane surface. The figure depicts the equilibrium orientational distribution of AmB polyol moieties with respect to the membrane normal (z-axis) in a system where a single AmB tetramer was placed in the water phase close to the membrane surface. The orientations assumed by the molecule are close to uniform, as indicated by the good agreement between the actual distribution (green) and the ideal uniform one (black). Horizontal orientations (close to 90°) can be additionally favored by the excluded volume effect as a result of the confinement of an elongated molecule between the membrane surface and its periodic image.

basis of differences in the average fluorescence lifetimes coded by colors of FLIM images (Figures 2−4).

Further insight into the role of the lipid environment on the molecular organization of AmB is provided by the detailed analysis of the fluorescence-lifetime components of AmB in all the experimental systems studied, as presented in Figure 7. The uniform distribution of colors in the FLIM images recorded from all the systems analyzed implies a homogeneous distribution of the molecular-organization forms of AmB in the lipid membranes formed with pure components and the membranes modified with sterols. On the other hand, it has to be mentioned that some images collected during our experiments have shown the distinctive nanoscale structures of AmB, characterized by short fluorescence lifetimes (below 1 ns) and assigned to aggregates, both in GUVs formed with pure lipids and in GUVs formed with lipids modified with sterols (Figure S2). Moreover, in the case of liposomes formed with POPC, often one can observe the formation of relatively large extramembranous structures characterized by short fluorescence lifetimes and exceptionally high fluorescence-anisotropy values (Figure 4 and S3). The fluorescence lifetimes determined selectively in those nanostructures of AmB (0.6 ns) do not correspond directly to the fluorescence-lifetime-value diagnostic for AmB tetramers formed in the water phase (0.35 ns),[35] which suggests that the structures observed (Figures S2 and S3) do not represent aggregates of AmB immobilized at the liposome surface from the water phase but rather multicomponent structures formed in situ and composed of AmB and either lipids, sterols, or mixtures of lipids and sterols. Such molecular-organization forms of AmB can represent extramembranous supramolecular structures, referred to as "sponges", reported previously.[12,17] The effect of sterols on the molecular organization of AmB seems to be clearly manifested by differences in fluorescence lifetimes. As can be seen, the fluorescence-lifetime components resolved in the systems composed of lipids differ not only in the amplitudes of individual components but also in the fluorescence-lifetime-component values in the systems composed of both lipids and sterols (Figure 7). The short-lifetime component, assigned to the aggregated forms of the drug (0.6 ns), appeared longer than the structures formed in the water phase (0.35 ns),[35] whereas the long-lifetime component assigned to the antiparallel AmB dimer (6.8 ns)[35] appeared even longer upon binding to the lipid membrane (∼9 ns). The 1.8 ns component represents a parallel dimer, and the 3 ns components represent monomers[35] (see Figure S4).

Table 1. Orientation of the Transition Dipole of Amphotericin B in Different Molecular-Organization Forms with Respect to the Axis Normal to the Plane of the Lipid Membranes[a]

	orientation angle [°]								
composition	DPPC	DPPC + Ergo	DPPC + Chol	DMPC	DMPC + Ergo	DMPC + Chol	POPC	POPC + Ergo	POPC + Chol
tetramer or trimer	56.6 ± 3.7	47.5 ± 4.8	51.0 ± 5.2	54.0 ± 1.6	42.7 ± 2.3	49.5 ± 5.8	56.7 ± 3.0	47.8 ± 3.8	59.3 ± 5.6
dimer, parallel	58.8 ± 4.6	49.8 ± 5.3	46.9 ± 4.3	46.8 ± 1.4	56.9 ± 2.6	43.6 ± 6.9	53.0 ± 3.3	47.2 ± 2.2	58.6 ± 6.7
monomer	57.0 ± 4.0	50.9 ± 3.8	46.9 ± 5.6	54.8 ± 3.5	57.3 ± 4.7	58.4 ± 3.7	56.4 ± 3.2	49.5 ± 6.7	56.9 ± 4.6
dimer, antiparallel	57.3 ± 4.7	48.1 ± 7.8	51.9 ± 5.2	56.5 ± 3.9	56.6 ± 5.4	60.4 ± 2.5	53.7 ± 4.1	46.8 ± 1.8	58.0 ± 5.3

[a]The results are the arithmetic means ± SD from three to nine determinations based on individual liposomes.

DOI: 10.1021/acs.molpharmaceut.8b00572
Mol. Pharmaceutics 2018, 15, 4202−4213

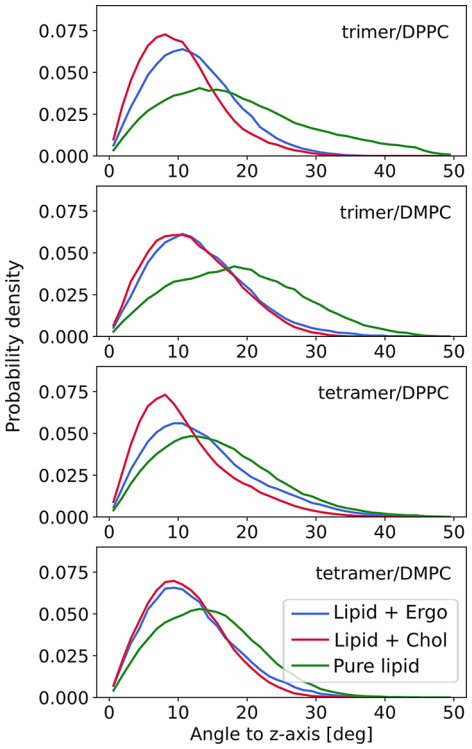

Figure 6. Orientation of AmB molecules in membrane-embedded oligomers. Tilt-angle distributions of polyene moieties are shown for AmB oligomers (trimers and tetramers) embedded in bilayers of different compositions: 30% Ergo, 30% Chol, or sterol-free with either DMPC or DPPC as the main bilayer component. The sterol-induced ordering effect is clearly visible and slightly stronger with Chol than with Ergo. Also, ordering is more pronounced for tetramers than for trimers, suggesting that higher oligomers can be more rigidly oriented in the membrane. The tilt angle is defined as the angle between the longest axis of the macrolide ring and the membrane normal (*z*-axis).

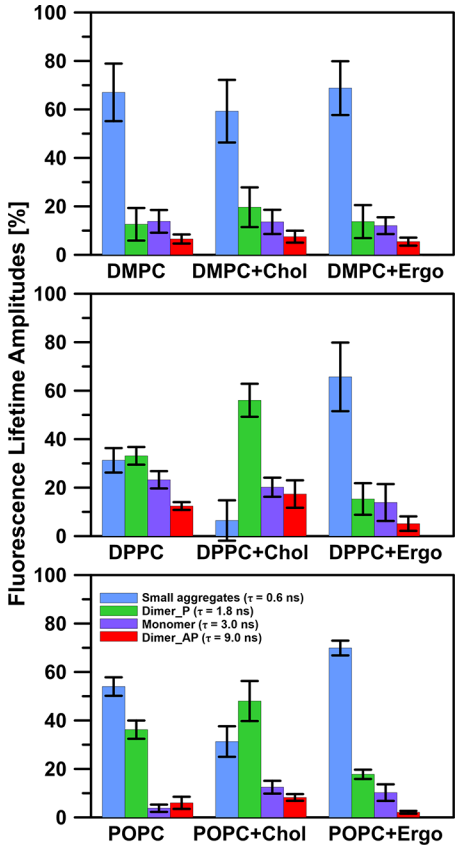

Figure 7. Distribution of relative fluorescence-lifetime amplitudes of AmB in liposomes of different compositions. Four fluorescence lifetimes were resolved, 0.6, 1.8, 3.0, and 9.0 ns, and have been assigned to AmB small aggregates (indicated), parallel dimers (Dimer_P), monomers, and antiparallel dimers (Dimer_AP) on the basis of the literature data.[35] Liposomes were formed with DMPC (upper panel), DPPC (middle panel), or POPC (lower panel) and with pure lipids or with lipids also containing 30 mol % cholesterol (Chol) or ergosterol (Ergo). The results represent the arithmetic means ± SD from 7 to 15 experiments.

To additionally dissect contributions corresponding to vertically and horizontally orientated drug molecules, we exploited the photoselection effect to separately record fluorescence-emission spectra from single liposomes formed with different lipids in the regions representing AmB fractions oriented parallel and perpendicular to the membrane normal, as presented in Figure 8. As can be seen, the spectra representing both fractions are very similar in the cases of DPPC and DMPC, which corroborates a heterogeneous and broad distribution of orientation angles of AmB in pure-lipid systems without sterols. The changes observed in the case of the membranes formed with POPC are consistent with heterogeneous orientations of different spectral forms representing supramolecular structures of AmB in this system, even without sterols (Figure 8C). The principal fluorescence maximum, visible in all the spectra at ∼460 nm, represents most probably the (0−0) emission from the lowest electronic singlet excited band (S1, 2^1A_g, see Figure S4).[35] Fluorescence emissions originating from this energy level correspond mostly to monomeric AmB[35] but can also represent different molecular-organization forms of AmB, giving rise to excitonic levels localized above S1 on the energy scale, providing highly efficient relaxation to the lowest excited state. The differences in the shapes of the emission spectra recorded in individual lipids represent, most probably, differences in the fractions of various molecular-organization forms in those systems (see Figure 7). The striking difference between the fluorescence-emission spectra of AmB recorded in other solvents and systems (e.g., refs 35 and 36) and those recorded directly from molecules associated with lipid membranes formed with pure lipids is the lack of the long-wavelength bands in the spectra recorded in the present study. This shows that large aggregated structures, giving rise to low-energy-emission bands, are not associated with lipid membranes, remain in the water phase, or are effectively dissolved in the lipid phase.

The most pronounced differences between the fluorescence-emission spectra of AmB located in the plane and those located perpendicular to the membrane plane can be observed in the case of lipids modified with sterols (see Figures 9 and 10). The molecular structures of AmB formed in the Ergo-containing membranes give rise to spectral bands that are, in general, shifted toward longer wavelengths (see Figure 9). In this respect, a band between 460 and 550 nm is representative; it is particularly enhanced in Ergo-containing membranes formed with DPPC (Figure 9D) and POPC (Figure 9F). A fluorescence-lifetime component of 0.6 ns, dominant in this system (Figure 7), represents the kinetics of de-excitation of AmB in this particular molecular-organization form. On the other hand, the incorporation of AmB into lipid membranes formed with the same lipid but modified with Chol (DPPC

DOI: 10.1021/acs.molpharmaceut.8b00572
Mol. Pharmaceutics 2018, 15, 4202−4213

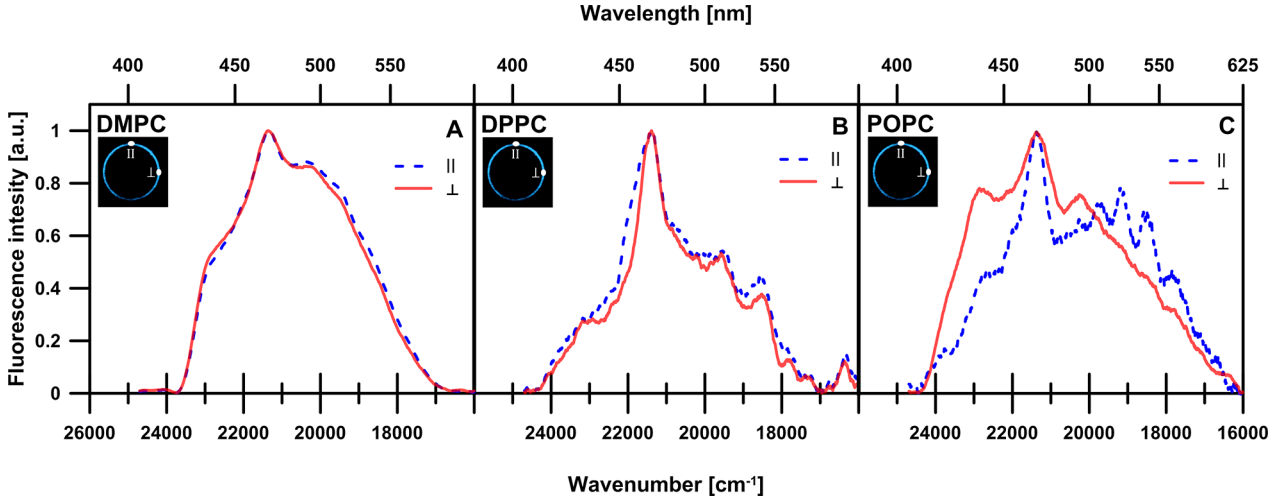

Figure 8. Fluorescence-emission spectra recorded from single AmB-containing liposomes. Liposomes were formed with (A) DMPC, (B) DPPC, or (C) POPC. In each case, two spectra were recorded from the places marked in the scheme presented in the inset, representing fractions of molecules oriented perpendicular (⊥) or parallel (||) with respect to the membrane plane as a result of photoselection.[17] The fluorescence spectrum recorded from an extramembranous AmB structure is also presented in panel C.

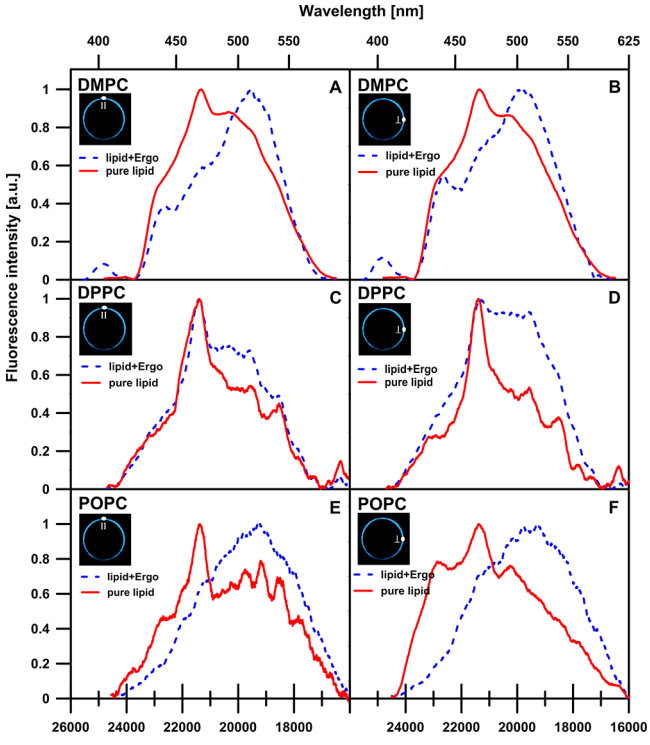

Figure 9. Fluorescence-emission spectra recorded from single AmB-containing liposomes. Liposomes were formed with DMPC (upper panels), DPPC (middle panels), or POPC (lower panels) and with pure lipids (solid lines) or with the addition of 30 mol % Ergo (dashed lines). The portions of the liposomes at which the spectra were recorded are marked in the insets.

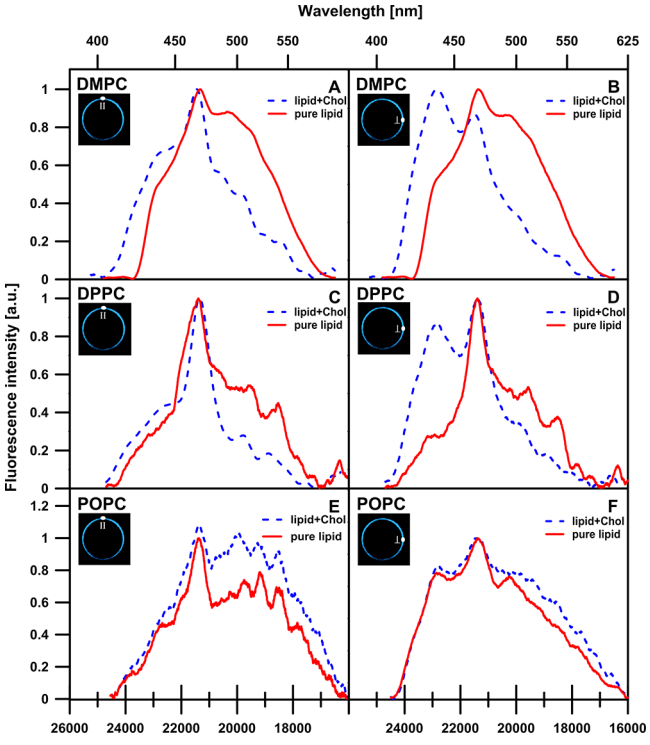

Figure 10. Fluorescence-emission spectra recorded from single AmB-containing liposomes. Liposomes were formed with DMPC (upper panels), DPPC (middle panels), or POPC (lower panels) and with pure lipids (solid lines) or with the addition of 30 mol % Chol (dashed lines). The portions of the liposomes at which the spectra were recorded are marked in the insets.

+Chol) results in the formation of molecular structures characterized by the short-wavelength fluorescence-emission band between 416 and 455 nm, which almost as intensive as the band attributed to the S1−S0 transition with a maximum at 460 nm (Figure 10D), at the expense of the molecular forms characterized by the long-wavelength fluorescence emission and assigned to small AmB aggregates (see Figure S4). The particularly low concentration of aggregated structures of AmB in the DPPC membranes containing Chol also can be directly concluded from the low relative amplitude of the fluorescence-lifetime component (τ = 0.6 ns, see Figure 7). The long-wavelength spectral forms that are particularly abundant in the DPPC−Ergo system are preferentially oriented perpendicular with respect to the membrane plane (Figure 9D). Interestingly, very little changes can be observed in the spectra representing vertically oriented AmB in the POPC membranes modified

DOI: 10.1021/acs.molpharmaceut.8b00572
Mol. Pharmaceutics 2018, 15, 4202−4213

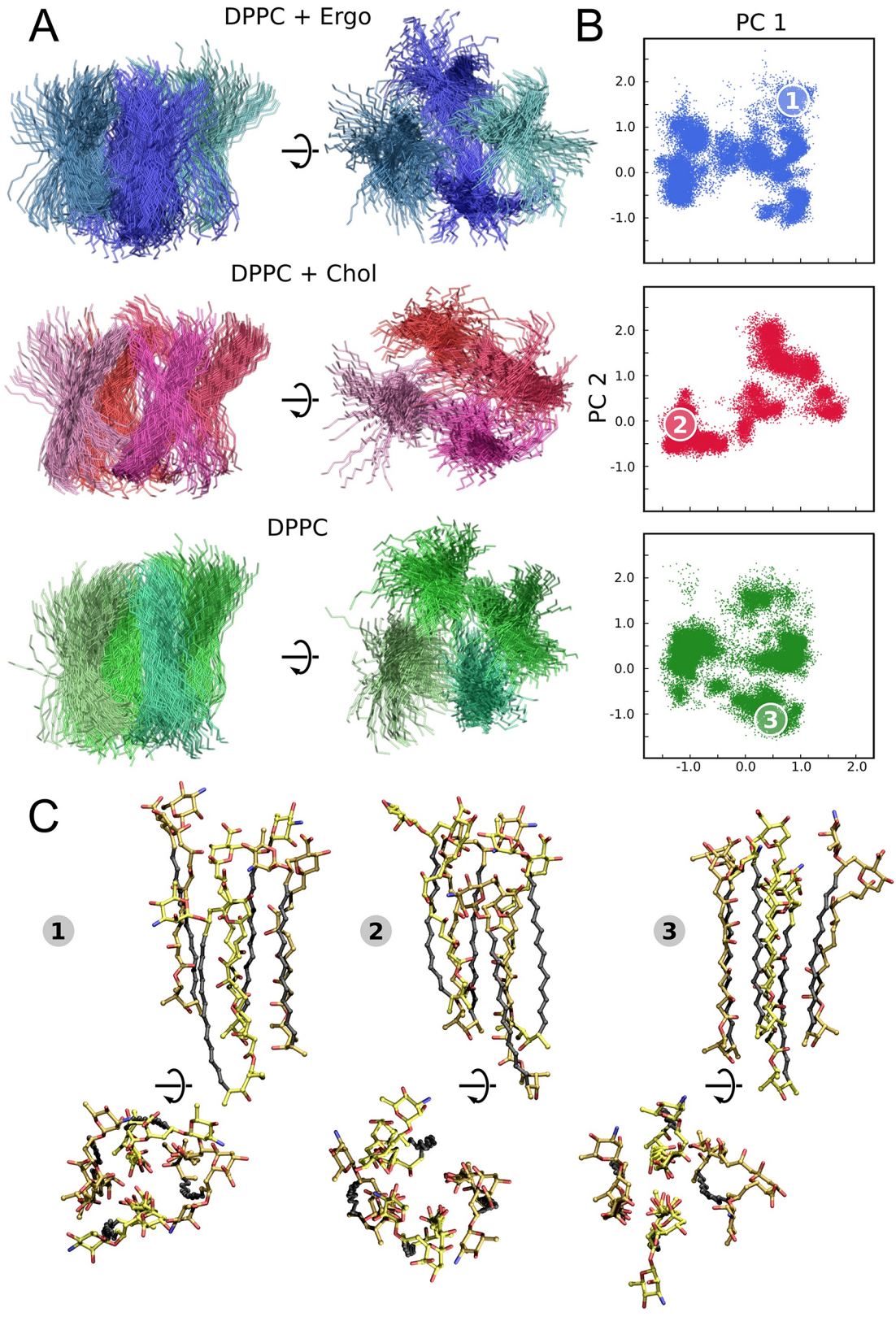

Figure 11. Conformational ensembles of AmB oligomers. (A) Side (left) and top (right) views of the ensembles of chromophore conformations depicting the conformational heterogeneity observed in the MD simulations of the AmB tetramers in DPPC with 30% Ergo, with 30% Chol, or without sterols. AmB molecules in a tetramer can be seen to twist around each other in either right- or left-handed directions (see, for example, DPPC+Chol). (B) Principal-component analysis (PCA) of tetramer structures in bilayers of different compositions (see the Experimental Methods for details). (C) Representative structures corresponding to the extreme clusters revealed by the PCA analysis, marked as 1, 2, and 3 in panel B. Side and top views are shown, with the chromophore (polyene moiety) marked in black.

DOI: 10.1021/acs.molpharmaceut.8b00572
Mol. Pharmaceutics 2018, 15, 4202−4213

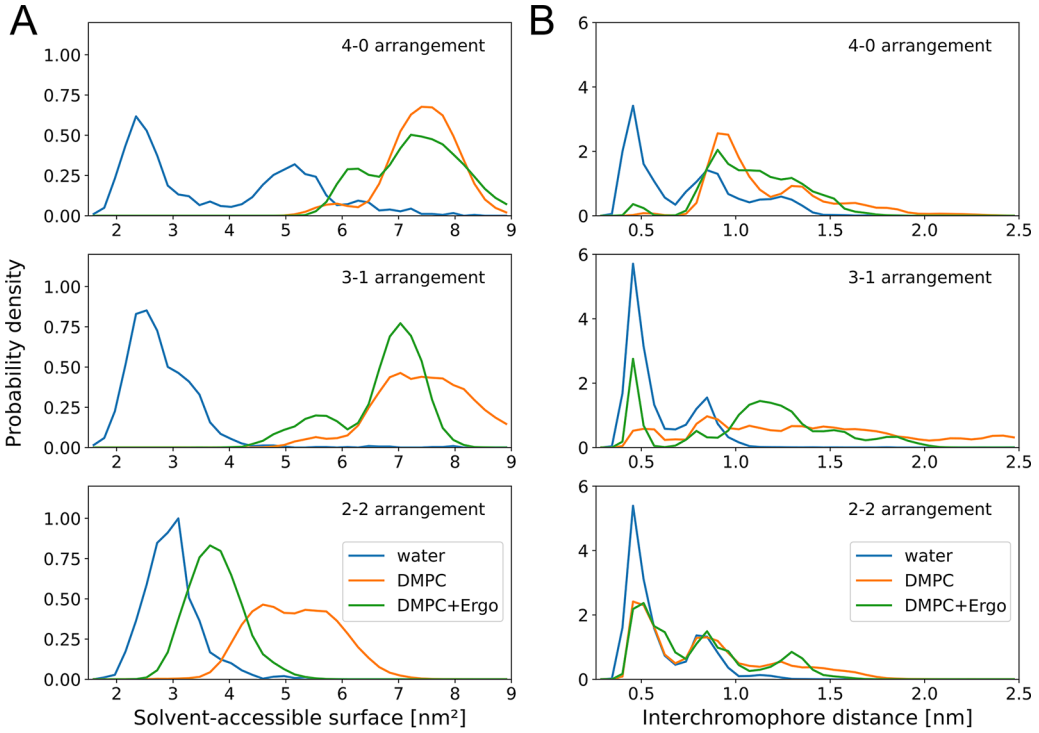

Figure 12. Changes in the structural properties of AmB tetramers upon transfer from the water to the lipid environment. Distributions of (A) the solvent-accessible surface areas (SASAs) of the polyene moieties and (B) the interchromophore distances for AmB tetramers in the water phase and in sterol-free (DMPC) and sterol-rich (DMPC+Ergo) bilayers. Three different tetramer arrangements are considered: all parallel (4−0), one antiparallel to three others (3−1), and two pairs of molecules in opposite directions (2−2). In all cases, a similar trend is visible: in water, the chromophores tend to cluster close together (hence their low SASAs and low interchromophore distances), whereas in the membrane, they face outward toward the hydrophobic-bilayer core (high SASAs and high interchromophore distances).

with Chol (Figure 10F). Such an effect suggests relatively broad orientational distribution both in the system without and in the system with the sterol. A very similar conclusion was drawn above on the basis of the fluorescence-detected linear dichroism data presented in Table 1.

By interpreting fluorescence-lifetime components and differences in the shapes of the recorded emission spectra in the context of individual oligomeric states, we implicitly assume that these signals represent differences in the molecular organization of the drug and not different dynamically switching conformations of the individual oligomeric states. To test this assumption, we used MD simulations to investigate the dynamics of AmB tetramers embedded in the DPPC bilayer, as shown in Figure 11. When projected on the plane of the greatest structural variability, the obtained ensemble of oligomers in different membrane systems can be seen to span a narrow and overlapping space of possible conformations. This result strongly suggests that there is no consistent variability in the structural properties of the membrane-bound oligomers, indicating that the variation in the observed FLIM data indeed reflects different stoichiometry of oligomers and not different conformations of the same oligomeric state.

At the same time, the structural ensemble (and hence the observed fluorescence pattern) is not solely determined by the oligomeric state but also by the medium in which oligomers form. For this reason, we resolved the structural differences between small AmB oligomers located in the water phase and the bilayer by simulating the dynamics of AmB tetramers in both environments and subsequently analyzing the equilibrium distributions of both the interchromophore distances and solvent-accessible surface areas (SASAs) of the chromophores. The results, presented in Figure 12, consistently showed that tetramers in water have lower SASAs and lower mean interchromophore distances than those in either pure DMPC or DMPC−sterol systems, except for the 2−2 arrangement, which failed to equilibrate fully within the simulation time scale (the time series did not reach a plateau). This overall trend can be easily explained by the amphipathic structure of AmB, which causes the polyol part to move outward in water and the polyene part to be exposed to the environment in a bilayer. The presence of such a transition is also consistent with the experimentally observed shift toward longer fluorescence lifetimes upon insertion in the membrane.

Combined, these experimental and simulational data provide further support for the intramembrane localization and vertical orientation of supramolecular structures of AmB in the sterol-containing membranes.[17] The fact that such structures have been assigned, on the basis of the results of orientation analysis, as adopting the in-membrane localization has two important implications. The first one is that potentially, such structures can be involved in facilitating the leaking of small ions through the membrane. The second implication is that AmB structures localized within the membranes affect the structural properties of lipid bilayers. In fact, such a mechanism can be very clearly visible from an analysis of the results of differential-scanning calorimetry (DSC). Figures 13 and S5 present the thermograms of different lipid systems modified with sterols and AmB. The general conclusion from the results of the DSC analyses is that the presence of AmB shifts the main phase transition considerably toward higher temperatures in the case of pure-lipid systems (with both DMPC and

DOI: 10.1021/acs.molpharmaceut.8b00572
Mol. Pharmaceutics 2018, 15, 4202−4213

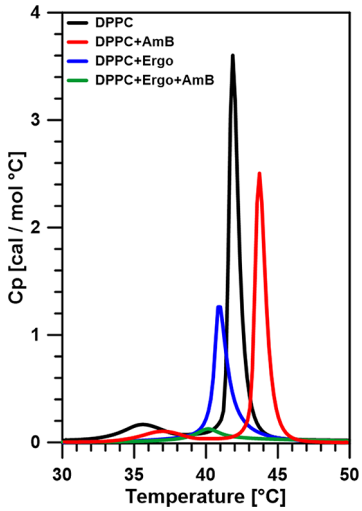

Figure 13. DSC thermograms of liposomes. Liposomes were formed either with pure DPPC or with DPPC containing 10 mol % Ergo (DPPC+Ergo) and scanned as controls or exposed to interaction with AmB (DPPC+AmB or DPPC+Ergo+AmB). The results of the examination of the same systems but containing 30 mol % Ergo or Chol are shown in Figure S5.

DPPC) but shifts the phase-transition temperature in the opposite direction and almost abolishes the phase transition in lipid systems containing sterols. Qualitatively, very similar effects from AmB on the phase transition of DPPC membranes have been observed previously in AmB and sterol-containing liposomes formed from the component mixtures.[37] Such an observation is consistent with the model, according to which AmB molecular structures are anchored in the polar membrane zone, most probably via a hydrogen-bond network, in the case of pure-lipid systems. The same structures can adopt the in-membrane location in the presence of sterol in the lipid phase. Such a localization results apparently in a dramatic disturbance of the lipid-bilayer structure, manifested by the critical decrease in cooperativity of the phase transition.

DISCUSSION

Fluorescence-emission- and fluorescence-lifetime-based analyses were applied to analyze the molecular organization and localization of the polyene antibiotic AmB in a single lipid membrane and to image the distribution of the drug in such a system. An approach based on microscopic imaging on the nanoscale provides solid ground for analysis of molecular mechanisms associated with the effect of AmB directly on lipid membranes. This is due to the fact that molecules of the drug present in the samples but not interacting directly with lipids (e.g., in the water phase) did not interfere with the analysis of individual lipid-membrane structures. As can be seen from the analysis of the absorption spectra of the liposome suspension (Figure 1), molecules of AmB form molecular aggregates in the water phase. The position of the most blue-shifted absorption maximum at 332 nm suggests that the pool of aggregated forms of AmB may be constituted, to a large extent, of tetramers characterized by the main absorption band at 335 nm and a fluorescence lifetime of τ = 0.350 ns.[35] Interestingly, the fluorescence-emission component characterized selectively by this fluorescence lifetime has not been identified in the analyses of all the individual liposomes. This result indicates that this particular molecular-organization form of AmB, present in the water phase, undergoes reorganization while interacting with lipid membranes, as was indeed confirmed by our molecular simulations. Interestingly, another relatively short fluorescence-lifetime component can be resolved (0.6 ns) in particular in the samples demonstrating low-energy fluorescence-emission bands (see Figures 7 and 9). It is highly probable that this long-wavelength fluorescence-emission band, characterized by the short-lifetime component, represents small aggregates of AmB, readily formed as hybrid structures with other constituents of the membranes. Such a conclusion corroborates the fact that the large aggregated structures formed with pure AmB and giving rise to the absorption band in the region of 330 nm are not present in the absorption spectra of the liposome suspension (Figure 1, lower panel). The main absorption bands in the liposome-suspension spectrum, centered at 341 and 388 nm, correspond very well to the high excitonic bands previously assigned to the parallel (340 nm) and antiparallel (388 nm) dimers of pure AmB[35] (see also Figure S4). The results of the fluorescence-lifetime analysis (Figure 7) confirm the presence of the spectral forms characteristic for those structures: parallel dimers (1.8 ns) and antiparallel dimers associated with membranes (9.0 ns). The differences in the fluorescence-lifetime components observed in the sterol-containing systems imply that sterols do not only change the distribution of AmB molecules between the molecular-organization forms but also influence the molecular organization of the drug, very likely via the formation of heterocomplexes with AmB and therefore by affecting the distances between the chromophores. This conclusion is again supported by our simulations, which show the high structural similarity between oligomers formed in different types of membranes. Combined analysis of the results of the fluorescence lifetimes and molecular orientations of AmB leads to the conclusion that the presence of sterols in the lipid phase of liposomes promotes the incorporation of small aggregates into the membranes (see the scheme in Figure 14). Such a mechanism seems to have a significant biological consequence for two basic reasons. The first one is the presence of a molecular structure inside the membrane, through which the process of uncontrolled ion transport may be facilitated. This sterol-induced ordering of AmB oligomers along the bilayer normal, observed in our simulations, should indeed facilitate ion leakage by stabilization of the trans-membrane pore formed by the drug molecules. The second reason is directly related to the effects of the physical properties of the lipid phase, in particular in the membranes containing sterols, as manifested by the complete loss of the cooperativity of the main phase transition, visible in the DSC experiments (Figures 13 and S5). This suggests that small molecular aggregates of AmB can be primarily responsible for the biological activity of this drug, via the disintegration of Ergo-containing fungal biomembranes and via effects on the Chol-containing biomembranes of a human. Fortunately for the antibiotic selectivity toward fungi, the presence of Ergo promotes the formation of small aggregates of AmB in the environment of lipid membranes, in contrast to the effect of Chol, which apparently acts in the opposite direction (see Figure 7). This effect is particularly pronounced in the model membranes formed with DPPC and POPC (Figure 6). The thicknesses of the hydrophobic cores of the lipid bilayers formed with DPPC and POPC (~3 nm)[38,39] are comparable to the thicknesses of the hydrophobic cores of most biomembranes (~3 nm).[40] Such an agreement makes this

DOI: 10.1021/acs.molpharmaceut.8b00572
Mol. Pharmaceutics 2018, 15, 4202−4213

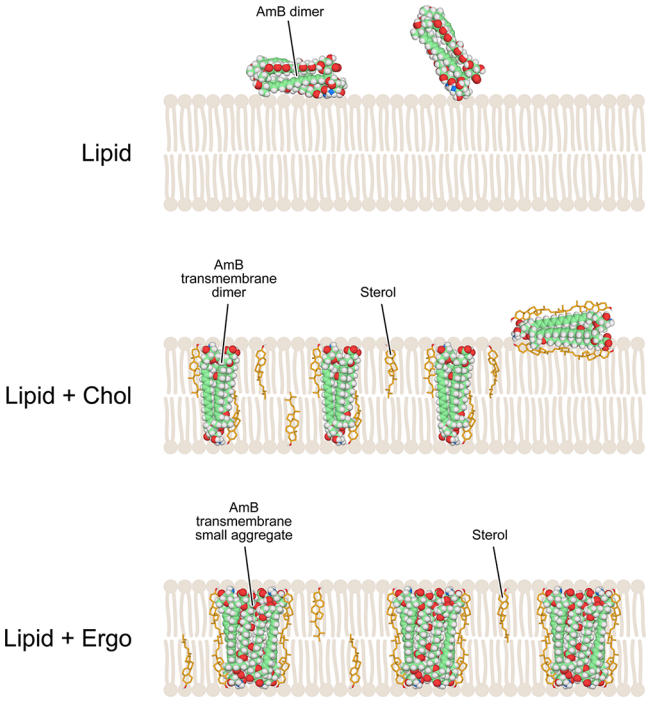

Figure 14. Scheme summarizing the molecular organization, localization, and orientation of amphotericin B with respect to lipid membranes. The model is based on the results of fluorescence-lifetime imaging, fluorescence-emission spectroscopy, fluorescence-detected linear dichroism, DSC, and molecular-dynamics simulations and is representative of liposomes formed with DPPC and DOPC.

system well suited to model the interaction of AmB with the lipid phase of natural membranes. The fact that tetramers of AmB and other small aggregates characterized by relatively fast fluorescence decay (τ = 0.6 ns), such as trimers, are preferentially formed in the presence of Ergo suggests the direct presence of the molecules of this particular sterol in the molecular structures observed. Although the spectroscopy and optical-microscopy data may not precisely address the problem of the stoichiometry of such heterocomplexes formed with AmB and Ergo, the results strongly indicate such a possibility.

Taking into consideration the results of the present study, one can conclude that formulations of the antibiotic AmB with minimized toxicity to patients but retained pharmacological activity toward fungi shall be composed of dimers of the drug that are incapable of forming higher aggregates. Such requirements can be satisfied, for example, in antibiotic-delivery systems based on Chol-containing liposomes formed with DPPC or POPC (see Figure 7). In this respect, it is worth mentioning that Chol was found to markedly reduce ion permeability induced by membrane-bound AmB.[41]

Interestingly, the formation of relatively large extramembranous AmB structures has been observed in the model membrane systems, in particular with an unsaturated lipid (POPC, Figures 4 and S3). The fluorescence lifetime determined for AmB in such structures (~0.6 ns) was different from that of aggregates of the drug formed in the water phase (0.35 ns), which implies that lipid molecules are involved in the formation of such structures. Moreover, the AmB-orientation data (Table 1) suggest that in the case of the Chol-containing membranes, the sterol influences the formation of molecular assemblies of AmB, which are not bound into the hydrophobic membrane core. This implies that one of the possible mechanisms of toxicity of the antibiotic can be based directly upon binding, reorientation, and relocation of Chol molecules in biomembranes (see Figure 14).

■ ASSOCIATED CONTENT

Supporting Information

The Supporting Information is available free of charge on the ACS Publications website at DOI: 10.1021/acs.molpharmaceut.8b00572.

Chemical structure of amphotericin B, additional FLIM images of liposomes, energy-level diagram of amphotericin B, and additional thermograms of liposomes (PDF)

■ AUTHOR INFORMATION

Corresponding Authors

*E-mail: wieslaw.gruszecki@umcs.pl (W.I.G.).
*E-mail: jacek.czub@pg.edu.pl (J.C.).

ORCID

Jacek Czub: 0000-0003-3639-6935
Wieslaw I. Gruszecki: 0000-0002-8245-3913

Author Contributions

□E.G. and M.W. contributed equally to this work. E.G. contributed to the experimental part, and M.W. contributed to the molecular-dynamics-computational part.

Notes

The authors declare no competing financial interest.

■ ACKNOWLEDGMENTS

The research was financed by the National Science Centre of Poland (NCN) under project 2015/19/B/NZ7/02159. The research was carried out with equipment purchased thanks to the financial support of the European Regional Development Fund in the framework of the Development of Eastern Poland Operational Programme. This research was supported in part by PL-Grid Infrastructure and the TASK Computer Centre.

■ ABBREVIATIONS USED

AmB , amphotericin B; Chol , cholesterol; Ergo , ergosterol; DMPC , dimyristoylphosphatidylcholine; DPPC , dipalmitoylphosphatidylcholine; POPC , 1-palmitoyl-2-oleoylphosphatidylcholine; FLIM , fluorescence-lifetime-imaging microscopy; DSC , differential-scanning calorimetry; GUV , giant unilamellar vesicle

■ REFERENCES

(1) Hamill, R. J. Amphotericin B formulations: a comparative review of efficacy and toxicity. *Drugs* **2013**, *73* (9), 919−34.

(2) Bicanic, T.; Bottomley, C.; Loyse, A.; Brouwer, A. E.; Muzoora, C.; Taseera, K.; Jackson, A.; Phulusa, J.; Hosseinipour, M. C.; van der Horst, C.; Limmathurotsakul, D.; White, N. J.; Wilson, D.; Wood, R.; Meintjes, G.; Harrison, T. S.; Jarvis, J. N. Toxicity of amphotericin B deoxycholate-based Induction therapy in patients with HIV-associated cryptococcal meningitis. *Antimicrob. Agents Chemother.* **2015**, *59* (12), 7224−31.

(3) Endo, M. M.; Cioffi, A. G.; Burke, M. D. Our Path to Less Toxic Amphotericins. *Synlett* **2016**, *27* (3), 337−354.

(4) Walker, L.; Sood, P.; Lenardon, M. D.; Milne, G.; Olson, J.; Jensen, G.; Wolf, J.; Casadevall, A.; Adler-Moore, J.; Gow, N. A. R. The viscoelastic properties of the fungal cell wall allow traffic of AmBisome as intact liposome vesicles. *mBio* **2018**, *9* (1), No. e02383-17.

(5) Liu, M.; Chen, M.; Yang, Z. Design of amphotericin B oral formulation for antifungal therapy. *Drug Delivery* **2017**, *24* (1), 1−9.

DOI: 10.1021/acs.molpharmaceut.8b00572
Mol. Pharmaceutics 2018, 15, 4202−4213

(6) Neumann, A.; Baginski, M.; Czub, J. How do sterols determine the antifungal activity of amphotericin B? Free energy of binding between the drug and its membrane targets. *J. Am. Chem. Soc.* **2010**, *132* (51), 18266−72.
(7) Umegawa, Y.; Matsumori, N.; Oishi, T.; Murata, M. Ergosterol increases the intermolecular distance of amphotericin B in the membrane-bound assembly as evidenced by solid-state NMR. *Biochemistry* **2008**, *47* (51), 13463−13469.
(8) Vertut-Croquin, A.; Bolard, J.; Chabbert, M.; Gary-Bobo, C. Differences in the interaction of the polyene antibiotic amphotericin B with cholesterol- or ergosterol-containing phospholipid vesicles. A circual dichroism and permeability study. *Biochemistry* **1983**, *22*, 2939−2944.
(9) De Kruijff, B.; Demel, R. A. Polyene antibiotic-sterol interaction in membranes of Acholeplasma laidlawii cells and lecithin liposomes; III Molecular structure of the polyene antibiotic-cholesterol complex. *Biochim. Biophys. Acta, Biomembr.* **1974**, *339*, 57−70.
(10) Ermishkin, L. N.; Kasumov, K. M.; Potzeluyev, V. M. Single ionic channels induced in lipid bilayers by polyene antibiotics amphotericin B and nystatine. *Nature* **1976**, *262* (5570), 698−9.
(11) Neumann, A.; Czub, J.; Baginski, M. On the possibility of the amphotericin B-sterol complex formation in cholesterol- and ergosterol-containing lipid bilayers: A molecular dynamics study. *J. Phys. Chem. B* **2009**, *113* (48), 15875−15885.
(12) Anderson, T. M.; Clay, M. C.; Cioffi, A. G.; Diaz, K. A.; Hisao, G. S.; Tuttle, M. D.; Nieuwkoop, A. J.; Comellas, G.; Maryum, N.; Wang, S.; Uno, B. E.; Wildeman, E. L.; Gonen, T.; Rienstra, C. M.; Burke, M. D. Amphotericin forms an extramembranous and fungicidal sterol sponge. *Nat. Chem. Biol.* **2014**, *10* (5), 400−6.
(13) Chudzik, B.; Koselski, M.; Czurylo, A.; Trebacz, K.; Gagos, M. A new look at the antibiotic amphotericin B effect on Candida albicans plasma membrane permeability and cell viability functions. *Eur. Biophys. J.* **2015**, *44* (1−2), 77−90.
(14) Herec, M.; Dziubinska, H.; Trebacz, K.; Morzycki, J. W.; Gruszecki, W. I. An effect of antibiotic amphotericin B on ion transport across model lipid membranes and tonoplast membranes. *Biochem. Pharmacol.* **2005**, *70* (5), 668−675.
(15) Herec, M.; Islamov, A.; Kuklin, A.; Gagos, M.; Gruszecki, W. I. Effect of antibiotic amphotericin B on structural and dynamic properties of lipid membranes formed with egg yolk phosphatidylcholine. *Chem. Phys. Lipids* **2007**, *147* (2), 78−86.
(16) Tutaj, K.; Szlazak, R.; Szalapata, K.; Starzyk, J.; Luchowski, R.; Grudzinski, W.; Osinska-Jaroszuk, M.; Jarosz-Wilkolazka, A.; Szuster-Ciesielska, A.; Gruszecki, W. I. Amphotericin B-silver hybrid nanoparticles: synthesis, properties and antifungal activity. *Nanomedicine* **2016**, *12* (4), 1095−1103.
(17) Grudzinski, W.; Sagan, J.; Welc, R.; Luchowski, R.; Gruszecki, W. I. Molecular organization, localization and orientation of antifungal antibiotic amphotericin B in a single lipid bilayer. *Sci. Rep.* **2016**, *6*, 32780.
(18) Ricci, M.; Oliva, R.; Del Vecchio, P.; Paolantoni, M.; Morresi, A.; Sassi, P. DMSO-induced perturbation of thermotropic properties of cholesterol-containing DPPC liposomes. *Biochim. Biophys. Acta, Biomembr.* **2016**, *1858* (12), 3024−3031.
(19) Cheng, C. Y.; Song, J. S.; Pas, J.; Meijer, L. H. H.; Han, S. G. DMSO Induces Dehydration near Lipid Membrane Surfaces. *Biophys. J.* **2015**, *109* (2), 330−339.
(20) Valeur, B. *Molecular Fluorescence. Pronciples and Applications*; Wiley-VCH: Weinheim, 2006.
(21) Jo, S.; Lim, J. B.; Klauda, J. B.; Im, W. CHARMM-GUI Membrane Builder for mixed bilayers and its application to yeast membranes. *Biophys. J.* **2009**, *97* (1), 50−8.
(22) Bonomi, M.; Branduardi, D.; Bussi, G.; Camilloni, C.; Provasi, D.; Raiteri, P.; Donadio, D.; Marinelli, F.; Pietrucci, F.; Broglia, R. A.; Parrinello, M. PLUMED: A portable plugin for free-energy calculations with molecular dynamics. *Comput. Phys. Commun.* **2009**, *180* (10), 1961−1972.
(23) Zielinska, J.; Wieczor, M.; Baczek, T.; Gruszecki, M.; Czub, J. Thermodynamics and kinetics of amphotericin B self-association in aqueous solution characterized in molecular detail. *Sci. Rep.* **2016**, *6*, 19109.
(24) Klauda, J. B.; Venable, R. M.; Freites, J. A.; O'Connor, J. W.; Tobias, D. J.; Mondragon-Ramirez, C.; Vorobyov, I.; MacKerell, A. D.; Pastor, R. W. Update of the CHARMM all-atom additive force field for lipids: Validation on six lipid types. *J. Phys. Chem. B* **2010**, *114* (23), 7830−7843.
(25) Neumann, A.; Wieczor, M.; Zielinska, J.; Baginski, M.; Czub, J. Membrane sterols modulate the binding mode of amphotericin B without affecting its affinity for a lipid bilayer. *Langmuir* **2016**, *32* (14), 3452−3461.
(26) Van der Spoel, D.; Lindahl, E.; Hess, B.; Groenhof, G.; Mark, A. E.; Berendsen, H. J. C. GROMACS: Fast, flexible, and free. *J. Comput. Chem.* **2005**, *26* (16), 1701−1718.
(27) Berendsen, H. J.; Postma, J. V.; van Gunsteren, W. F.; DiNola, A. R. H. J.; Haak, J. R. Molecular dynamics with coupling to an external bath. *J. Chem. Phys.* **1984**, *81*, 3684−3690.
(28) Van Gunsteren, W. F.; Berendsen, H. J. C. A Leap-Frog algorithm for stochastic dynamics. *Mol. Simul.* **1988**, *1* (3), 173−185.
(29) Hess, B. P-LINCS: A parallel linear constraint solver for molecular simulation. *J. Chem. Theory Comput.* **2008**, *4* (1), 116−122.
(30) Miyamoto, S.; Kollman, P. A. Settle - an analytical version of the Shake and Rattle algorithm for rigid water models. *J. Comput. Chem.* **1992**, *13* (8), 952−962.
(31) Darden, T.; York, D.; Pedersen, L. Particle Mesh Ewald - an N.Log(N) method for Ewald sums in large systems. *J. Chem. Phys.* **1993**, *98* (12), 10089−10092.
(32) McGibbon, R. T.; Beauchamp, K. A.; Harrigan, M. P.; Klein, C.; Swails, J. M.; Hernandez, C. X.; Schwantes, C. R.; Wang, L. P.; Lane, T. J.; Pande, V. S. MDTraj: A modern open library for the analysis of molecular dynamics trajectories. *Biophys. J.* **2015**, *109* (8), 1528−1532.
(33) Humphrey, W.; Dalke, A.; Schulten, K. VMD: Visual molecular dynamics. *J. Mol. Graphics* **1996**, *14* (1), 33−38.
(34) Barwicz, J.; Gruszecki, W. I.; Gruda, I. Spontaneous organization of amphotericin B in aqueous medium. *J. Colloid Interface Sci.* **1993**, *158*, 71−76.
(35) Starzyk, J.; Gruszecki, M.; Tutaj, K.; Luchowski, R.; Szlazak, R.; Wasko, P.; Grudzinski, W.; Czub, J.; Gruszecki, W. I. Self-association of amphotericin B: Spontaneous formation of molecular structures responsible for the toxic side effects of the antibiotic. *J. Phys. Chem. B* **2014**, *118* (48), 13821−13832.
(36) Wasko, P.; Luchowski, R.; Tutaj, K.; Grudzinski, W.; Adamkiewicz, P.; Gruszecki, W. I. Toward understanding of toxic side effects of a polyene antibiotic amphotericin B: Fluorescence spectroscopy reveals widespread formation of the specific supramolecular structures of the drug. *Mol. Pharmaceutics* **2012**, *9* (5), 1511−1520.
(37) Fournier, I.; Barwicz, J.; Tancrede, P. The structuring effects of amphotericin B on pure and ergosterol- or cholesterol-containing dipalmitoylphosphatidylcholine bilayers: a differential scanning calorimetry study. *Biochim. Biophys. Acta, Biomembr.* **1998**, *1373* (1), 76−86.
(38) Li, L. B. B.; Vorobyov, I.; Allen, T. W. The role of membrane thickness in charged protein-lipid interactions. *Biochim. Biophys. Acta, Biomembr.* **2012**, *1818* (2), 135−145.
(39) Guo, Y. C.; Pogodin, S.; Baulin, V. A. General model of phospholipid bilayers in fluid phase within the single chain mean field theory. *J. Chem. Phys.* **2014**, *140* (17), 174903.
(40) van Meer, G.; Voelker, D. R.; Feigenson, G. W. Membrane lipids: where they are and how they behave. *Nat. Rev. Mol. Cell Biol.* **2008**, *9* (2), 112−24.
(41) Matsuoka, S.; Murata, M. Cholesterol markedly reduces ion permeability induced by membrane - bound amphotericin B. *Biochim. Biophys. Acta, Biomembr.* **2002**, *1564*, 429−434.

DOI: 10.1021/acs.molpharmaceut.8b00572
Mol. Pharmaceutics 2018, 15, 4202−4213